Proceeding of the 13^{th} International Symposium on Experimental Robotics,
Québec, QC, Canada, June 17–21, 2012.

On the Development of a Programmable Inertia Generator

C. Gosselin, A. Lecours, T. Laliberté and F. Lessard
Département de génie mécanique, Université Laval, Québec, Qc, Canada
gosselin@gmc.ulaval.ca, alexandre.lecours.1@ulaval.ca, thierry@gmc.ulaval.ca,
frederic.lessard.2@ulaval.ca

Abstract This paper presents a preliminary investigation on a one-degree-of-freedom programmable inertia generator. An inertia generator is a hand-held haptic device that has a programmable inertia. By moving internal masses in reaction to accelerations induced by the user, the effective intertia of the device is modified in order to render a prescribed perceived inertia. In this paper, a one-degree-of-freedom device with one internal moving mass is proposed. The dynamic modelling of the system is first presented. Then, a controller is designed to produce the appropriate motion of the internal mass in reaction to the acceleration induced by the user. A prototype is presented and experimental results are discussed.

1 Introduction

It is common, for training or entertainment purposes, to actively prescribe the dynamics rendered by a robotic system. For instance, impedance control is used in haptics or physical human-robot interaction (pHRI) in order to simulate virtual environments. This approach can be implemented using fixed-base haptic devices which are controlled to produce a desired behaviour (see for instance [7] and many others).

In interactive systems (e.g. computer games), hand-held devices are also often used. These devices are typically passive [13] and are unable to produce kinesthetic feedback. However, as shown in [1], [11], it is possible to include moving masses in hand-held devices in order to produce an illusion of an external force. This approach can also be used with rotating mechanisms in order to produce the illusion of an external moment [2], [15].

The work reported in this paper addresses a similar but different challenge. The long-term objective of this initiative is to design a hand-held device that has a programmable inertia. The effective inertia of such a device is modified by moving internal masses in reaction to the accelerations imparted to the hand-held system by the user. Using this approach, the inertia perceived by the user manipulating the

hand-held device can be prescribed arbitrarily, within the physical constraints of the mechanical system.

In this paper, a preliminary investigation on a one-degree-of-freedom (one-dof) device is reported. The main objective of this first phase of the work is to assess the feasibility of the concept. In order to vary the perceived inertia, a moving mass is mounted on a slider within the manipulated one-dof physical interface. By moving the internal mass in reaction to an accelerometer signal, a prescribed effective inertia can be rendered. The paper is structured as follows: after providing a general description of the concept of inertia generator, the dynamic model of the one-dof mechanical system studied here is derived. Then, a controller is designed to produce the appropriate motion of the internal mass in reaction to the accelerations. A description of the physical one-dof prototype is then provided. Finally, experimental results are given and interpreted.

2 General Concept of Inertia Generator

The general concept of inertia generator is represented schematically in Fig. 1. Consider a box which is held by a user and inside of which a set of masses are mounted on actuated sliders or revolute joints. For example, three masses could be mounted on orthogonal actuated rails and three inertias could be mounted on orthogonal actuated pivots. Alternatively, one single rigid body could be attached to the end-effector of a 6-dof parallel mechanism that can produce translations and rotations of this mass in arbitrary directions. When the user imparts accelerations to the box, the latter are measured by a set of accelerometers and the masses are displaced in order to render a prescribed inertia. If the ratio of the moving masses to the mass of the frame of the box is large enough, accelerating the internal masses will produce a significant change in the external apparent inertia of the box. For instance, if the user is accelerating the box along the x axis and it is desired to render an inertia that is smaller to the physical inertia of the system, the mass(es) will be accelerated in the opposite direction in order to reduce the effective inertia. Similarly, if it is desired to render an inertia that is larger than that of the physical system, then the mass(es) will be moved in the direction of the acceleration imparted by the user in order to increase the apparent inertia.

The principle of the inertia generator is akin to that of motion simulators[14] and to that of acceleration compensation for vibration isolation[6, 5]. In such applications and in this work, the concept of *washout filter* is important[8]. The principle of the washout filter is to include a low-frequency command in the control loop that aims at bringing the mechanism to a *neutral* configuration so that it is ready for the next acceleration input. The neutral configuration is defined as one in which all directions of motion are feasible with approximately the same range of motion in all directions. This concept is discussed in the control section of the paper.

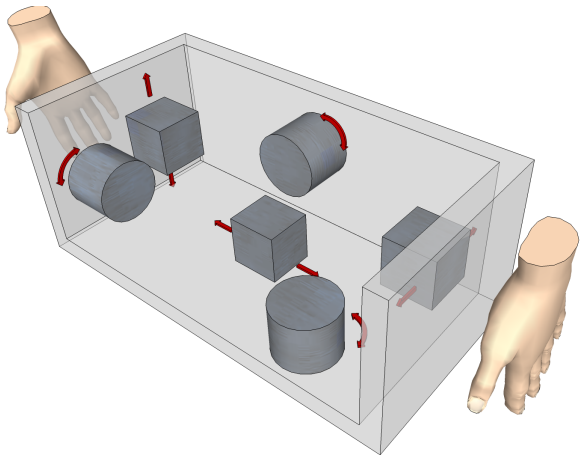

Fig. 1 Schematic representation of the concept of inertia generator.

3 Dynamic Modelling of a One-Degree-of-Freedom Inertia Generator

A schematic representation of the one-dof inertia generator is given in Fig. 2. The external frame of the device has a mass m_1 and is subjected to the external force F_1 applied by the user. It is assumed that the direction of motion is horizontal. An actuator is included in the device to move a second mass m_2 mounted on a slider attached to the frame of mass m_1. The force applied by the actuator on mass m_2 is noted F_2 while the friction force between the two masses is noted F_f. The position of the frame of the device with respect to a fixed inertial frame is noted x_1, the position of mass m_2 with respect to the inertial frame is noted x_2 and x_3 denotes the position of mass m_2 with respect to mass m_1. Therefore, one has

$$x_2 = x_1 + x_3, \qquad \ddot{x}_2 = \ddot{x}_1 + \ddot{x}_3. \tag{1}$$

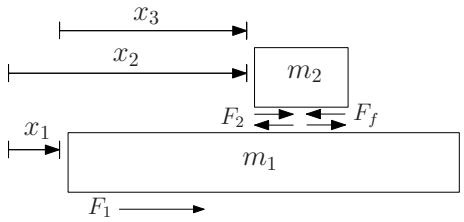

Fig. 2 Schematic representation of the one-dof inertia generator.

It is desired to render a prescribed inertia, noted m_a, when the user applies forces on the device. Therefore, the desired behaviour can be expressed as

$$F_1 = m_a \ddot{x}_1 \tag{2}$$

where $\ddot{x}_1$ is the acceleration of mass m_1 with respect to the fixed inertial frame.

Applying Newton's second law to each of the moving masses, one obtains

$$F_1 - (F_2 - F_f) = m_1 \ddot{x}_1 \tag{3}$$

$$F_2 - F_f = m_2 \ddot{x}_2 \tag{4}$$

where $\ddot{x}_2$ is the acceleration of mass m_2 with respect to the fixed inertial frame. Substituting eq.(1) into eqs.(3) and (4) and rearranging, one has

$$F_1 = (m_1 + m_2)\ddot{x}_1 + m_2 \ddot{x}_3 \tag{5}$$

$$F_2 = m_2 \ddot{x}_1 + m_2 \ddot{x}_3 + F_f. \tag{6}$$

Equations (5) and (6) represent the dynamics of the two-dof system comprising the mobile frame of mass m_1 and the sliding mass m_2. Referring to eq.(2), it is desired to obtain an expression for the force F_2 to be applied by the actuator in order to render the inertia m_a. To this end, eq.(2) is first substituted into eq.(5), which leads to

$$m_2 \ddot{x}_3 = (m_a - m_1 - m_2)\ddot{x}_1. \tag{7}$$

Substituting the latter equation into eq.(6) then leads to

$$F_2 = (m_a - m_1)\ddot{x}_1 + F_f. \tag{8}$$

Finally, eq.(7) is rearranged in order to determine the acceleration required at the actuator, namely by rewriting it as

$$\ddot{x}_{d3} = \frac{(m_a - m_1 - m_2)\ddot{x}_1}{m_2} \tag{9}$$

where $\ddot{x}_{d3}$ is the desired relative acceleration.

4 Controller Design

Based on the dynamic model presented in the previous section, a control scheme can be developed in order to render the prescribed inertia m_a. The system is designed to react to the acceleration of the moving frame of mass m_1. To this end, an accelerometer is mounted on the frame, which provides a measurement of its acceleration $\ddot{x}_1$. The control strategy is based on the combination of three terms, namely: a feedforward term (including friction compensation), a feedback term, and a washout term. Each of these contributions is now detailed.

4.1 Feedforward and Friction Compensation

The feedforward term is based on the dynamic model developed in the preceding section. Equation (8) is used to compute an estimation of the the force to be applied at the actuator based on the measured acceleration $\ddot{x}_1$ and on an estimation of the friction force F_f. A simple friction compensation can be written as:

$$F_f = f_c + f_v \tag{10}$$

where f_c and f_v are respectively the Coulomb and viscous friction forces with

$$f_c = c(1 - e^{-\alpha|\dot{x}_{d3}|})sign(\dot{x}_{d3}) \tag{11}$$

$$f_v = v\dot{x}_{d3} \tag{12}$$

where c is the Coulomb friction coefficient, v the viscous friction coefficient and α is a tuning parameter. The exponential term is used to reduce the chattering induced by friction compensation when the velocity is near zero. The desired velocity is used for friction compensation in order to reduce the command noise, although the measured velocity could also be used. Other more complex friction models could also be used (see for instance[16, 4, 3, 9, 10]), including stiction for example, but the simple friction compensation given in eqn. (10) provided good experimental results.

4.2 Feedback

The desired acceleration of mass m_2 can be computed using eq.(9). In order to achieve this relative acceleration, it would be possible to use a feedback control (e.g. PID control) with a relative acceleration measurement (e.g. accelerometer or second derivative of the position). However, acceleration control is not very practical mainly because the measured acceleration is known to be very noisy. Instead, velocity or position control can be implemented using an integration technique.

First, the discrete desired velocity required to render the desired acceleration is obtained with a zero-order-hold integration[1]:

$$\dot{x}_{d3}(k) = \dot{x}_{d3}(k-1) + \ddot{x}_{d3}(k)T_s \tag{13}$$

while the position is obtained by integrating a second time, namely:

$$x_{d3}(k) = x_{d3}(k-1) + \dot{x}_{d3}(k-1)T_s + \frac{1}{2}\ddot{x}_{d3}(k)T_s^2 \tag{14}$$

where T_s is the sampling period, k is the time step and x_{d3}, $\dot{x}_{d3}$ and $\ddot{x}_{d3}$ are respectively the desired position, velocity and acceleration.

[1] Alternatively, a bilinear discretization can be used.

One should note that this integration method is used to achieve acceleration control in physical human-robot interaction with admittance control schemes [12] and that, although it is preferable to use the desired velocity of the preceding step ($\dot{x}_{d3}(k-1)$), the measured velocity can alternatively be used in the above equations. The desired acceleration is then rendered using velocity or position control, which is more practical and can be achieved using a simple PID controller or more complex algorithms.

4.3 Washout

As explained in a preceding section, the goal of the washout filter is to ensure that the moving mass is kept as close as possible to its neutral position in order to be ready to accommodate arbitrary acceleration inputs. For the one-dof system studied here, this amounts to keeping mass m_2 as close as possible to its mid-range position in order to avoid the mechanical limits (end of stroke). To this end, a virtual spring-damper system modelled as follows is used:

$$F_w = -K_w(x_3 - x_w) - C_w\dot{x}_3 \tag{15}$$

where F_w stands for the washout force, K_w is the washout spring stiffness, C_w is the washout damping factor and x_w is the neutral position. The adjustment of the washout parameters is based on the analysis of the above second-order system. Knowing the mass to be moved m_2, one obtains

$$K_w = m_2\omega_w^2 \tag{16}$$

$$C_w = 2m_2\zeta_w\omega_w \tag{17}$$

where ω_w is the washout natural frequency and ζ_w is the damping factor. The washout natural frequency should be chosen low enough so that it does not significantly impact the rendering. On the other hand, it should be high enough to ensure that mass m_2 is kept close enough to its neutral position. In order to cope with this compromise, the washout natural frequency is adjusted according to the acceleration of the frame, $\ddot{x}_1$. The following heuristic rule is used:

$$\omega_w = \begin{cases} 0 & \text{if } |\ddot{x}_1| > \ddot{x}_{1t} \\ \omega_{w0}\left(1 - \frac{\ddot{x}_1^2}{\ddot{x}_{1t}^2}\right) & \text{otherwise.} \end{cases} \tag{18}$$

where ω_{w0} is the default washout natural frequency and $\ddot{x}_{1t}$ is an acceleration threshold above which the washout is deactivated. In this work, $\omega_{w0} = 2s^{-1}$ and $\ddot{x}_{1t} = 0.3ms^{-2}$ are used.

5 Experiments

The prototype used in the experiments reported in this paper is shown in Fig. 3. Mass m_1 consists of an aluminium plate equipped with wheels that can roll with low friction on a table top or on a floor. A DC motor is mounted on the plate together with a rail and pulleys while mass m_2 consists of a small steel plate and a trolley. The motion of mass m_2 is actuated by the DC motor and transmitted with a closed-loop belt. An accelerometer is mounted on the base plate in order to measure the acceleration of the frame, $\ddot{x}_1$. Also, an ATI MINI-40 force/torque sensor can be attached to the plate to measure the force F_1 applied by the user on the inertia generator and a second accelerometer can be mounted on mass m_2. The latter two measurements (force F_1 and acceleration $\ddot{x}_2$) are not used by the controller but only for experimental validation and analysis.

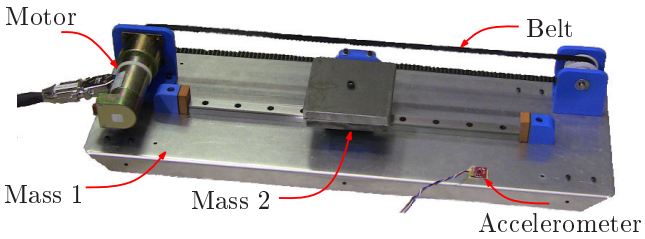

Fig. 3 Prototype of a one-dof inertia generator used in the experiments.

5.1 Model validation

A first experiment was performed in order to validate the dynamic model. In this experiment, the frame (mass m_1) is moved manually while the second mass (m_2) is free to slide on the rail. The interaction force (F_1) and the acceleration of each of the masses ($\ddot{x}_1$ and $\ddot{x}_2$) are measured. The measured accelerations are then compared with those computed using the measured force and the dynamic equations, in order to validate the model. The results are shown in Fig. 4. It can be observed that, although the results are not perfect, the model is sufficiently realistic to be used for control purposes.

5.2 Interaction experiments

Experiments were performed using the prototype described above, which has the following characteristics: $m_1 = 2.45kg$ and $m_2 = 2.32kg$, for a total moving mass

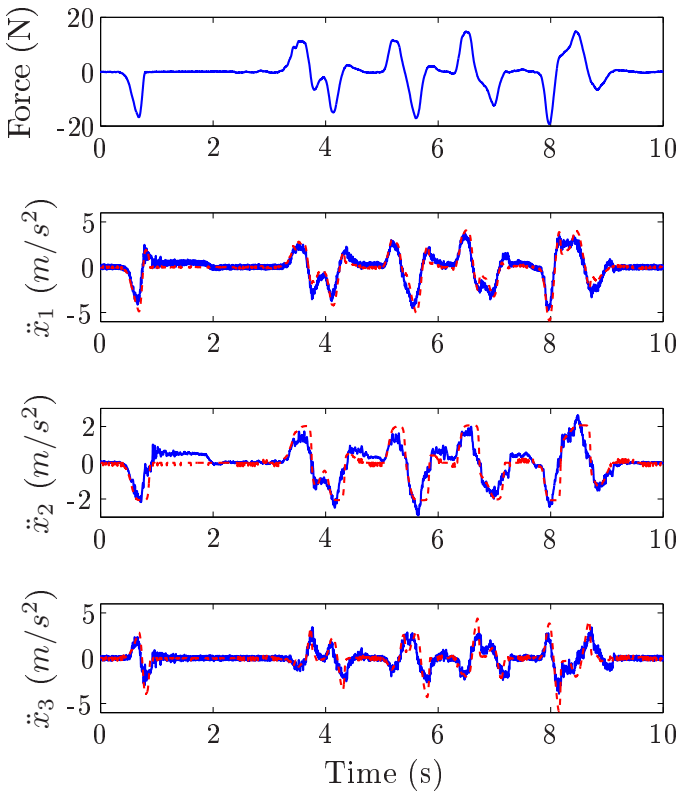

Fig. 4 Model validation. The solid lines represent measured quantities while the dashed lines represent accelerations computed using the dynamic model and the measured force.

of $4.77kg$. The effect of the prescribed inertia m_a is easily perceived by the user. However, in order to obtain quantitative data, the force and acceleration data were recorded in order to compare the results with the desired dynamics given by eqn. (2).

Figures 5 to 8 present the results obtained with a prescribed mass varying from $m_a = 1.25kg$ to $m_a = 6.00kg$. On the graphs, the force applied by the user (measured) is compared with the rendered force ($m_a\ddot{x}_1$) where $\ddot{x}_1$ is the measured acceleration.

6 Discussion

It can be observed from the experimental results that the prescribed inertia is generally well rendered. When the prescribed mass is close to the total mass $(m_1 + m_2)$, e.g., with $m_a = 4.77kg$, the results are obviously very good since the demands on the actuator are very low. These results can serve as a basis for the analysis of the results obtained in more demanding situations. Basically, if m_a is very close to $(m_1 + m_2)$,

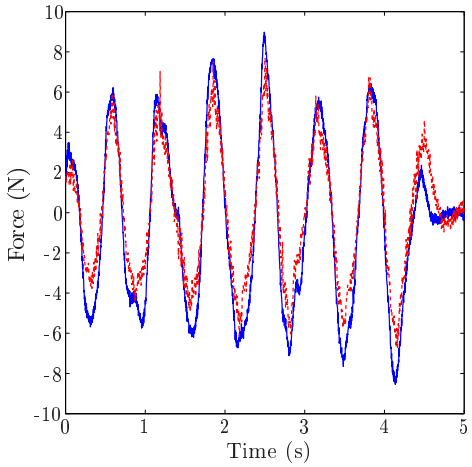

Fig. 5 Experimental results with $m_a = 1.25kg$. The solid line represents the measured force while the dashed line is the model force ($m_a\ddot{x}_1$) where $\ddot{x}_1$ is measured with an accelerometer.

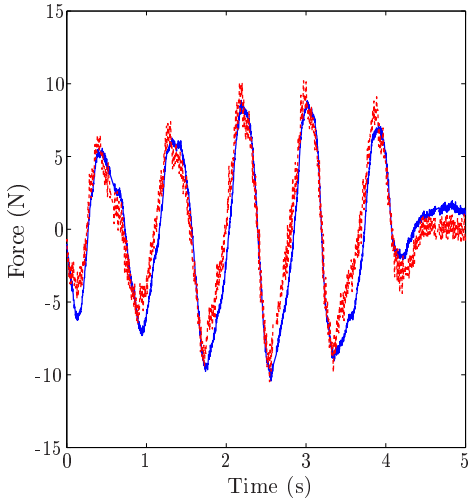

Fig. 6 Experimental results with $m_a = 2.45kg$. The solid line represents the measured force while the dashed line is the model force ($m_a\ddot{x}_1$) where $\ddot{x}_1$ is measured with an accelerometer.

the errors correspond to the estimation errors introduced by the control loop and the measurements themselves.

When the prescribed inertia is more significantly different from the total mass, the actuator is much more sollicited and the error tends to increase, as observed in Figs. 5 and 8. Nevertheless, the results are still acceptable, especially considering that the resolution capabilities of the user are limited. For example, with $m_a = 1.25kg$ (Fig. 5) the rendered mass is approximately $1.5kg$. It can be observed in the latter figure that the measured forces are slightly larger than the prescribed

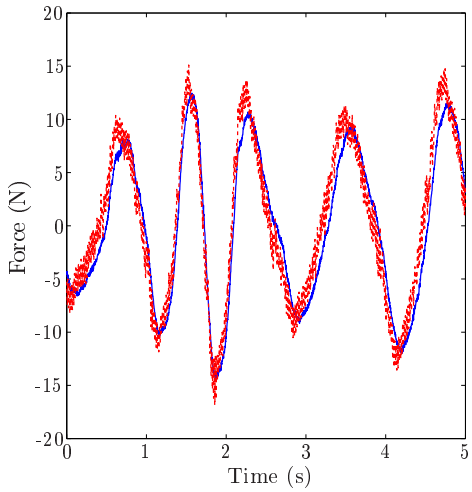

Fig. 7 Experimental results with $m_a = 4.77kg$. The solid line represents the measured force while the dashed line is the model force ($m_a\ddot{x}_1$) where $\ddot{x}_1$ is measured with an accelerometer.

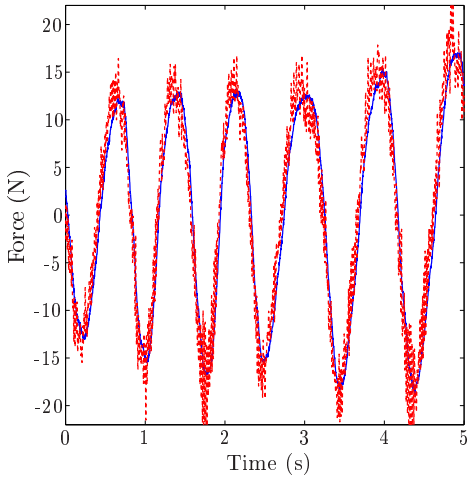

Fig. 8 Experimental results with $m_a = 6.00kg$. The solid line represents the measured force while the dashed line is the model force ($m_a\ddot{x}_1$) where $\ddot{x}_1$ is measured with an accelerometer.

forces. On the other hand, if the prescribed inertia is larger than the total mass, e.g., $m_a = 6.00kg$ (Fig. 8), the measured forces tend to be slightly smaller than the prescribed forces. These results demonstrate the feasibility of the concept. They also highlight the importance of properly selecting the ratio between m_2 and m_1, which in turn raises the issue of the power to mass ratio of the actuator. Ideally, the mass ratio (m_2/m_1) should be maximized so that the impact of the moving mass is maximized. One possible design avenue is to include the actuator in the moving mass in

order to increase the mass ratio. Using this principle, the power to mass ratio of the actuator becomes less important.

7 Conclusion

The concept of inertia generator was proposed in this paper. In a hand-held inertia generator, internal masses are moved in reaction to accelerations induced by the user such that the effective intertia of the device is modified in order to render a prescribed perceived inertia. This paper presented preliminary investigations on a one-dof inertia generator that has the capability to render a translational inertia in one direction. The dynamic model of the system was first derived. Based on this model, a controller was proposed that uses the measured acceleration of the frame as an input and determines the motion of the internal mass as an output. The controller is based on an integration of the acceleration signal in order to alleviate the difficulties associated with noisy accelerometer signals. A velocity or position control can therefore be used. Experimental results show that, although the power to mass ratio and the moving mass to frame mass ratio of the prototype are not high, the latter is capable of rendering a significant range of inertias. Future work includes the investigation of multi-dof inertia generators and the experimentation with more advanced prototypes.

Acknowledgements This work was supported by the Natural Sciences and Engineering Research Council of Canada (NSERC), by the Canada Research Chair program and by the Fonds de Recherche du Québec – Nature et Technologie (FRQNT). The authors would also like to thank Michaël Fortin for his help with some of the figures.

References

1. Amemiya, T., Ando, H., Maeda, T.: Lead-me interface for a pulling sensation from hand-held devices. ACM Transactions on Applied Perception (2008)
2. Ando, H., Sugimoto, M., Maeda, T.: Wearable moment display device for nonverbal communication. IEICE Transactions on Information and Systems E87-D (2004)
3. Armstrong-Helouvry, B., Dupont, P., Canudas De Wit, C.: A survey of models, analysis tools and compensation methods for the control of machines with friction. Automatica **30**(7), 1083–1138 (1994)
4. Cao, L., Schwartz, H.: Stick-slip friction compensation for pid position control. In: Proceedings of the American Control Conference (2000)
5. Ebert-Uphoff, I., Dang, A.: Active acceleration compensation for transport vehicles carrying delicate objects. IEEE Transactions on Robotics **20**(5), 830 – 839 (2004). DOI 10.1109/TRO.2004.832791
6. Graf, R., Dillmann, R.: Active acceleration compensation using a stewart platform on a mobile robot. In: Proc. 2nd Euromicro Workshop on Advanced Mobile Robots (1997)
7. Hannaford, B., Okamura, A.: Haptics. The Springer Handbook of Robotics, Siciliano and Khatib editors (2008)

8. Hassouneh, M., Lee, H., Abed, E.: Washout filters in feedback control: benefits, limitations and extensions. In: American Control Conference. Boston, USA (2004)
9. Kostic, D., de Jager, B., Steinbuch, M., Hensen, R.: Modeling and identification for high-performance robot control: an rrr-robotic arm case study. IEEE Transactions on Control Systems Technology **12**(6), 904 – 919 (2004). DOI 10.1109/TCST.2004.833641
10. Kostic, D., Steinbuch, M., de Jager, B.: Modeling and identification for robot motion control. Robotics and Automation Handbook (2004)
11. Laitinen, P., Mawnpaa, J.: Enabling mobile haptic design: piezoelectric actuator technology properties in hand-held devices. In: IEEE International Workshop on Haptic Audio Visual Environments and their Applications (2006)
12. Lecours, A., Mayer-St-Onge, B., Gosselin, C.: Variable admittance control of a four-degree-of-freedom intelligent assist device. In: IEEE International Conference on Robotics and Automation (2012)
13. Moen, J.: From hand-held to body-worn: embodied experiences of the design and use of a wearable movement-based interaction concept. In: First International Conference on Tangible and Embedded Interaction (2007)
14. Nahon, M., Reid, L.: Simulator motion-drive algorithms, a designer's perspective. Journal of Guidance, Control and Dynamics **13**(2), 356 – 362 (1990)
15. Nakamura, N., Fukui, Y.: Development of a force and torque hybrid display 'gyrocubestick'. In: IEEE World Haptics Conference (2006)
16. Canudas de Wit, C., Nol, P., Aubin, A., Brogliato, B.: Adaptive Friction Compensation in Robot Manipulators: Low Velocities. The International Journal of Robotics Research **10**(3), 189–199 (1991)